



Original article

Fluorescein-derived fluorescent probe for cellular hydrogen sulfide imaging



Hui-Ying Liu^{a,b,1}, Miao Zhao^{b,1}, Qing-Long Qiao^b, Hai-Jing Lang^b,
Jing-Zhe Xu^{a,*}, Zhao-Chao Xu^{b,*}

^a Department of Chemistry, Yanbian University, Yanji 133002, China

^b Dalian Institute of Chemical Physics, Chinese Academy of Sciences, Dalian 116023, China

ARTICLE INFO

Article history:

Received 24 January 2014

Received in revised form 24 March 2014

Accepted 4 April 2014

Available online 13 May 2014

Keywords:

Fluorescent probe

H₂S

Fluorescein

Thiolysis

ABSTRACT

In this work, a fluorescein-derived fluorescent probe for H₂S based on the thiolysis of dinitrophenyl ether is reported. This probe exhibits turn-on fluorescence imaging of H₂S in living cells and bulk solutions with excellent selectivity. The reaction mechanism was explained by means of absorption, fluorescence and HPLC–MS.

© 2014 Jing-Zhe Xu and Zhao-Chao Xu. Published by Elsevier B.V. on behalf of Chinese Chemical Society. All rights reserved.

1. Introduction

Hydrogen sulfide (H₂S) is well known as a toxic gas with the characteristic smell of rotten eggs. However, recent investigations have demonstrated that H₂S is the third most important gas transmitter for regulating cardiovascular, neuronal, immune, endocrine, and gastrointestinal systems, along with nitric oxide and carbon monoxide [1]. H₂S is produced endogenously in mammalian systems from L-cysteine in reactions catalyzed mainly by two pyridoxal-5'-phosphate-dependent enzymes, cystathionine β-synthase (CBS) and cystathionine γ-lyase (CSE) [2]. As a signal molecule, it modulates neuronal transmission [2], relaxes smooth muscle [3], regulates release of insulin [4] and is involved in inflammation [5]. The endogenous levels of H₂S are believed to be related to some diseases like Alzheimer's disease [6], Down's syndrome [7], diabetes [8] and liver cirrhosis [9]. Inhibitors of H₂S and H₂S donors have shown potential for therapeutic exploitation of H₂S [10] in animal disease models. Thus, visualization of the distribution and concentration of H₂S in living systems would be very important and helpful to elucidate the biological roles of H₂S.

Compared with reported methods such as colorimetric analysis, electrochemical analysis and gas chromatography, small molecule

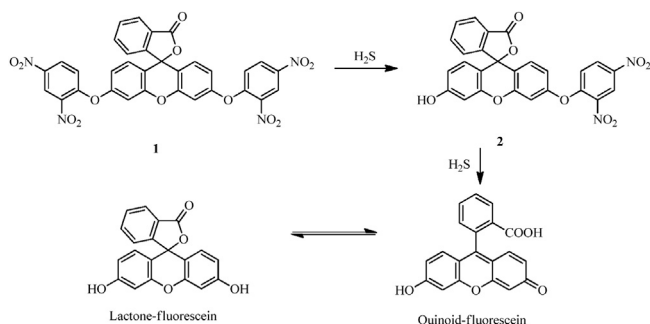
fluorescent probes offer higher sensitivity, real-time imaging, and higher spatiotemporal resolution, and have more potential to be a suitable tool. So far, a number of fluorescent probes for H₂S have been reported based on specific chemical reactions by taking advantage of the reducing or nucleophilic properties of H₂S [11–20]. Most of these probes display high selectivity for H₂S over other thiols such as cysteine due to the nature of reaction type recognition. However, in consideration of issues related specifically to application in biological tissues, more research is needed to improve the biocompatibility, absorption coefficient and fluorescent quantum yield, visible light excitation, photostability and signal-to-noise ratio (SNR) of H₂S fluorescent probes.

Fluorescein and its derivatives have been the most widely used class of organic dyes by biologists and chemists as safe fluorophores to design fluorescent probes, labels and immunological probes, for their excellent photophysical properties, such as high absorption coefficient, excellent fluorescent quantum yield and great photostability [21,22]. For example, folate conjugated to fluorescein iso-thiocyanate for targeting FR-α was reported as the first in-human use of intra-operative tumor-specific fluorescence imaging for real-time surgical visualization of tumor tissue in patients with suspected ovarian cancer [23]. Spirolactone derivatives are nonfluorescent and colorless, whereas ring-opening of the corresponding lactone gives rise to strong fluorescence and a green color [24]. Because of the high SNR turn-on response, taking advantages of the spiroring-opening mechanism, a large number of fluorescent probes have been developed for metal ions, anions and

* Corresponding authors.

E-mail addresses: jingzhex@ybu.edu.cn (J.-Z. Xu), zcxu@dicp.ac.cn (Z.-C. Xu).

¹ These authors contributed equally to this work.



Scheme 1. The reaction of compound **1** with H_2S .

small molecules in recent years [21,22,25]. Unfortunately, only a very few fluorescein-derived fluorescent probes have been designed on the basis of the spiroring-opening mechanism to image H_2S in living cells [26–29].

In this paper, we report a fluorescent probe **1** for detection of H_2S in aqueous solution and living cells (Scheme 1). The two hydroxyl groups of fluorescein were protected by dinitrophenyl ether, which acted as the H_2S reactive site [30,31]. The synthesis of **1** is quite straightforward and started from the cheap commercially available material fluorescein. The probe **1** was obtained in one step in high yield and characterized by ^1H NMR, ^{13}C NMR and HRMS. The experimental details are given in supporting materials.

2. Experimental

Unless otherwise stated, all reagents were purchased from commercial suppliers and used without further purification. ^1H NMR and ^{13}C NMR spectra were recorded on a VARIAN INOVA-400 spectrometer, using TMS as an internal standard. UV–visible spectra were collected on an Agilent Cary 60 UV/vis spectrophotometer. Fluorescence measurements were performed on an Agilent CARY Eclipse fluorescence spectrophotometer (Serial No. FL0812-M018). HPLC–MS analysis was performed on Agilent 6540 UHD Accurate-Mass Q-TOF LC/MS using an HPLC system composed of a pump (Agilent ZORBAX Eclipse Plus C18 2.1 mm \times 50 mm) and a DAD detector (254 nm).

Synthesis of 1: Fluorescein (332 mg, 1 mmol) and 1-bromine-2,4-dinitrobenzene (543 mg, 2.2 mmol, 2.2 equiv.) were added to 10 mL anhydrous DMF. After stirring at room temperature for 12 h, the solvent was removed under reduced pressure to obtain a pale solid, which was purified by silica gel column chromatography (PE: EA = 20:1) to afford desired product **1** as a light yellow solid (544 mg, 82% yield). The synthetic step of the sensor **1** was shown in Scheme S1 (Supporting information) and the NMR datas of the sensor **1** were shown in Figs. S1 and S2 (Supporting information). Mp 106–108 $^\circ\text{C}$. ^1H NMR (400 MHz, CDCl_3): δ 8.86 (d, 2H, $J = 2.8$ Hz), 8.40 (dd, 2H, $J = 9.2, 2.8$ Hz), 8.08 (d, 1H, $J = 7.6$ Hz), 7.79–7.69 (m, 2H), 7.26–7.20 (m, 3H), 6.96 (s, 1H), 6.94 (s, 1H), 6.87–6.84 (m, 2H). ^{13}C NMR (101 MHz, CDCl_3): δ 168.66, 155.77, 154.54, 152.24, 142.53, 140.30, 135.65, 130.53, 130.46, 128.97.

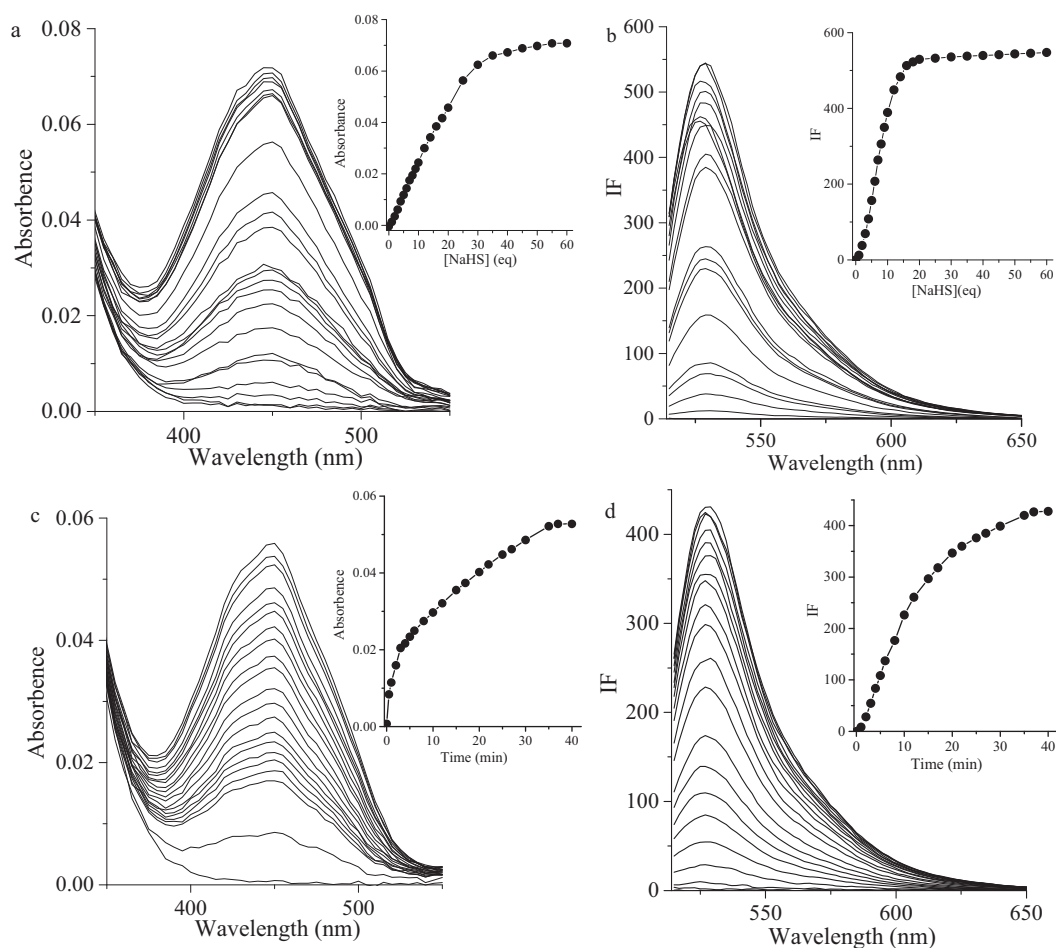


Fig. 1. (a) UV–vis absorption spectra of 10 $\mu\text{mol/L}$ compound **1** in the presence of 0–60 equiv. of H_2S in aqueous solution ($\text{CH}_3\text{CN}:\text{HEPES} = 6:4$, pH 7.4). (b) Fluorescent emission spectra of 10 $\mu\text{mol/L}$ compound **1** in the presence of 0–60 equiv. of H_2S in aqueous solution. (c) Time dependence of absorption profiles of **1** (10 $\mu\text{mol/L}$) with 30 equiv. H_2S . (d) Time dependence of fluorescence profiles of **1** (10 $\mu\text{mol/L}$) with 30 equiv. H_2S . $\lambda_{\text{ex}} = 450$ nm.

126.18, 125.61, 123.83, 122.17, 120.06, 116.92, 116.06, 108.46, 81.03. HRMS (ESI) calcd. for $C_{32}H_{17}N_4O_{13}$ $[MH^+]$ 665.0792, found 665.0794.

Culture of Hela cells and fluorescent imaging: Hela was cultured in Dulbecco's modified Eagle's medium (DMEM, Invitrogen) supplemented with 10% FBS (fetal bovine serum) in an atmosphere of 5% CO_2 and 95% air at 37 °C. The cells were seeded in 24-well flat-bottomed plates and then incubated for 48 h at 37 °C under 5% CO_2 . Probe **1** (5 μ mol/L) was then added to the cells and incubation for another 30 min followed. The cells were washed three times with phosphate-buffered saline (PBS). The cells were incubated with 100 μ mol/L of H_2S for 30 min. Fluorescence imaging was observed under a confocal microscope (Olympus FV1000) with a 60 \times objective lens.

3. Results and discussion

The absorption and fluorescence properties of **1** were tested in aqueous solution (CH_3CN :HEPES = 6:4, pH 7.4, 50 mmol/L). Compound **1** exhibited no absorption features in the visible region (Fig. 1a) and the solution of **1** was colorless (Fig. S3 in Supporting information). This meant that **1** adopted a closed lactone conformation which displayed no fluorescence (Fig. 1b). When 0–60 equiv. of NaHS was added to the solution of **1**, a new absorption band centered at 450 nm developed quickly (Fig. 1a) which induced the color change from colorless to yellow (Fig. S3). Under UV lamp irradiation, the changes of color before and after adding H_2S are also shown in Fig. S1. Simultaneously, the fluorescence emission band centered at 525 nm was observed and increased in intensity (Fig. 1b). We also found that if the concentration of NaHS was over 30 equiv., the reaction finished quickly (Insets in Fig. 1a and b). There was good linearity between the fluorescence intensity and the concentrations of H_2S in the range of 0–140 μ mol/L with a detection limit of 0.57 μ mol/L (Fig. S4 in Supporting information). Therefore, we used 30 equiv. of H_2S to examine the performance of **1** in all following experiments. The time-dependent fluorescence responses were next detected with the addition of 30 equiv. H_2S and the results showed that the reaction was completed within 40 min (Fig. 1c and d). Notably, the background fluorescence of **1** is very weak, and within minutes a high fluorescence increase is observed which relays the reaction of **1** with H_2S (Fig. 1d); therefore, the timescale allows **1** to sense H_2S in real-time intracellular imaging. The quantum yield of the probe

for detecting H_2S is 0.564 and the molar extinction coefficient is 7200 L/mol cm.

The fluorescence emission at 525 nm should belong to fluorescein in quinoid form, which resulted from the thiolysis of the dinitrophenyl ether by H_2S . To verify this mechanism, the reaction products of **1** with NaHS were analyzed by HPLC–MS (Fig. 2) and the corresponding MS data of the HPLC peaks have been shown in Fig. S5 (Supporting information). The absorption spectra of fluorescein in various solvents were also checked. As shown in Fig. S6 (Supporting information), the absorption peak in the visible region can only be found in protic solvents, which indicates that fluorescein forms a lactone in aprotic solvents, but a quinoid in protic solvents. From that, we can conclude that the peak in Fig. 2b belongs to fluorescein in its quinoid form. We also investigate the effect of pH on the absorption and fluorescence properties of the probe within pH range of 2.0–8.0. As shown in Fig. S7 (Supporting information), the changes of the pH affected the properties of the probe slightly. After reaction for 20 min, as shown in Fig. 2c, the product of fluorescein in its quinoid form was found, which confirmed the reaction mechanism. Interestingly, fluorescein in its lactone form and single dinitrophenyl ether protected compound **2** were also observed (Fig. S8 in Supporting information). After another 20 min, the reaction completed and the products contained fluorescein both in quinoid and lactone forms in a 1:4 ratio (Fig. 2d). From that, we may conclude that H_2S reacts with **1** to release dinitrophenyl ether one by one (Scheme 1). In pure CH_3CN , H_2S reacted with **1** quickly to form the fluorescent species of fluorescein in its quinoid form (Fig. S9 in Supporting information). However, in the next hour, the fluorescence decreased gradually due to the transformation of fluorescein from the quinoid form to the lactone form (Fig. S10 in Supporting information). It follows that the existence of fluorescein in its lactone form in the products should be ascribed to the large percentage of acetonitrile in mixture solution. Also, we may point out that compound **2** reacts with H_2S to produce fluorescein in its quinoid form firstly (Scheme 1).

The selectivity of the fluorescent response of **1** to H_2S was then examined. Fig. 3 shows the fluorescence response of **1** to various anions and sulfur-containing analytes in aqueous solutions (CH_3CN :HEPES = 6:4, pH 7.4). Selective and large fluorescent enhancements (FE, fold) were observed upon addition of NaHS to the solution of **1**. The addition of 100 equiv. of F^- , Cl^- , Br^- , ClO_4^- , HCO_3^- , NO_3^- , NO_2^- , PO_4^{3-} , HPO_4^{2-} , $H_2PO_4^-$, $P_2O_7^{4-}$, $S_2O_3^{2-}$, $S_2O_4^{2-}$, $S_2O_5^{2-}$, $S_2O_8^{2-}$, SO_3^- , N_3^- , SCN^- , CO_3^{2-} , CH_3COO^- , SO_4^{2-} ,

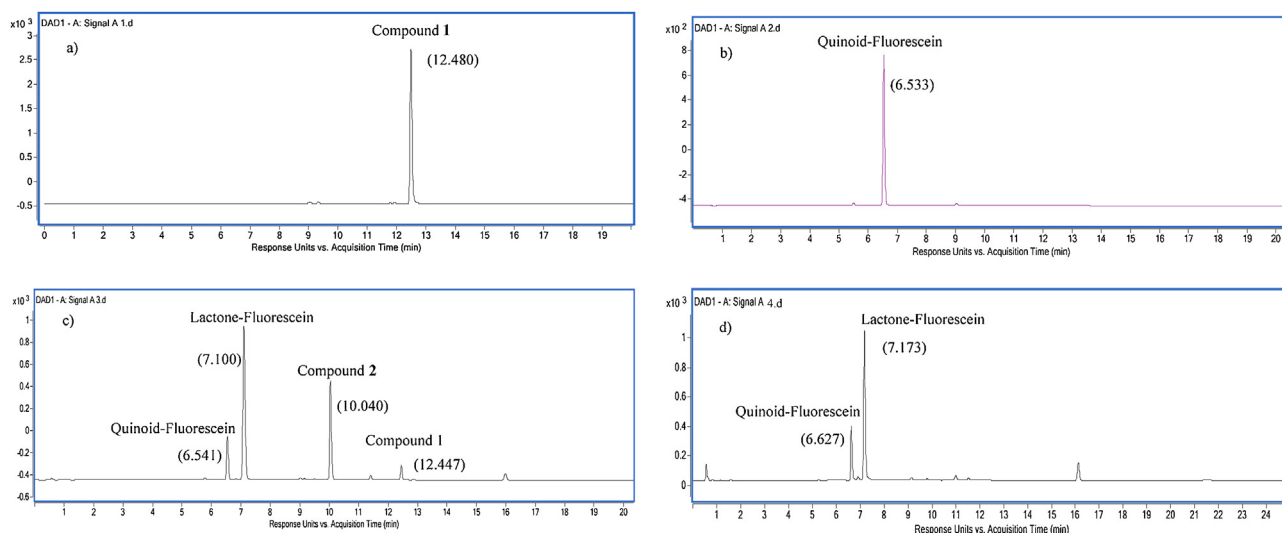


Fig. 2. HPLC of (a) Compound **1** (1.5 μ mol/L); (b) Fluorescein (3 μ mol/L); (c) the reaction product of **1** (1.5 μ mol/L) with NaHS (45 μ mol/L) after incubation of them for 20 min in CH_3CN /Water (6:4) solution; (d) the reaction product of **1** (1.5 μ mol/L) with NaHS (45 μ mol/L) after incubation of them for 40 min in CH_3CN /Water (6:4) solution.

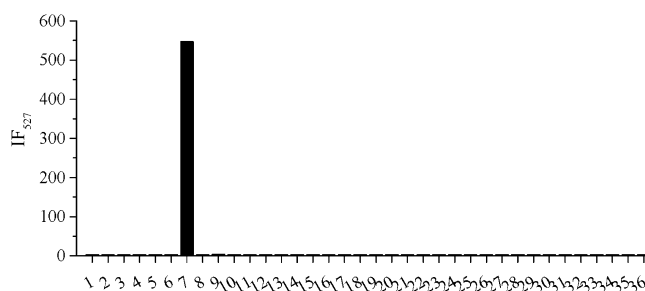


Fig. 3. Fluorescence responses of 10 $\mu\text{mol/L}$ **1** to various analytes in aqueous solution. Excitation at 450 nm. Bars represent the final fluorescence intensity of **1** with 1 mmol/L analytes over the original emission of free **1**. (1) Br^- ; (2) Cl^- ; (3) ClO^- ; (4) CN^- ; (5) CO_3^{2-} ; (6) cysteine; (7) NaHS ; (8) F^- ; (9) GSH; (10) H_2PO_4^- ; (11) HCO_3^- ; (12) homo-Cys; (13) $\text{HP}_2\text{O}_7^{3-}$; (14) HPO_4^{2-} ; (15) HSO_3^- ; (16) HSO_4^- ; (17) I^- ; (18) ascorbic acid; (19) N_3^- ; (20) citric acid; (21) hydrogen citrate; (22) dihydrogen citric acid; (23) No; (24) NO_2^- ; (25) NO_3^- ; (26) OAc^- ; (27) $\text{P}_2\text{O}_7^{4-}$; (28) PO_4^{3-} ; (29) $\text{S}_2\text{O}_4^{2-}$; (30) $\text{S}_2\text{O}_5^{2-}$; (31) $\text{S}_2\text{O}_8^{2-}$; (32) SCN^- ; (33) SO_4^{2-} ; (34) SO_3^{2-} ; (35) $\text{S}_2\text{O}_3^{2-}$; (36) *N*-acetyl cysteine.

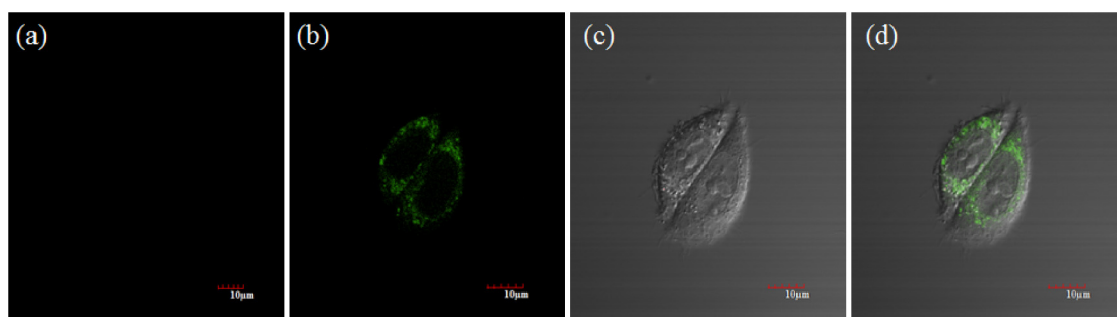


Fig. 4. Fluorescence images of HeLa cells incubated with 5 $\mu\text{mol/L}$ **1** and H_2S . Cells treated with **1** (a) in the absence and (b) presence of 100 $\mu\text{mol/L}$ of H_2S incubated for 30 min; (c) bright field; (d) merged images of (b) and bright field. Scale bars = 10 $\mu\text{mol/L}$.

HSO_4^- , citrate, hydrogen citrate, dihydrogen citrate, ascorbic acid, *L*-cysteine, homocysteine, *L*-glutathione and *N*-acetyl-*L*-cysteine produced only a nominal change in the fluorescence spectra of **1**. Therefore the probe **1** has a very high selectivity for H_2S .

We next tested the ability of **1** to be used to visualize H_2S in live cells. HeLa cells were incubated with **1** (5 $\mu\text{mol/L}$) for 30 min and exhibited no fluorescence (Fig. 4a). Then the cells were incubated with 100 $\mu\text{mol/L}$ NaHS , a concentration of H_2S comparable with physiological H_2S levels, and after 30 min they displayed enhanced green fluorescence (Fig. 4b). The cytotoxicity of **1** was examined toward HeLa cells by a MTT assay (Fig. S11 in Supporting information). The results showed that 95% HeLa cells survived after 12 h (5 mmol/L **1** incubation), and after 24 h the cell viability remained at $\sim 90\%$, demonstrating that **1** was of low toxicity toward cultured cell lines. These experiments indicate that **1** can act as a fluorescent probe to detect H_2S in living cells.

4. Conclusion

In conclusion, we have reported a fluorescein-derived fluorescent probe **1** for H_2S based on the thiolysis of dinitrophenyl ether. Due to rapid conversion to the fluorescent species of fluorescein in its quinoid form, a large fluorescence increase is obtained with emission centered at 525 nm in aqueous solution. The probe has a high selectivity for H_2S over competitive analytes. This probe is applicable to H_2S detection in live cell imaging. The successful application of our probe to detect cellular H_2S will help to study the biological role of H_2S and encourage the appearance of new H_2S probes suitable for cell imaging.

Acknowledgments

We thank financial supports from the National Natural Science Foundation of China (No. 21276251), Ministry of Human Resources and Social Security of PRC, the 100 talents program funded by

Chinese Academy of Sciences, and State Key Laboratory of Fine Chemicals of China (No. KF1105).

Appendix A. Supplementary data

Supplementary data associated with this article can be found, in the online version, at <http://dx.doi.org/10.1016/j.cclet.2014.05.010>.

References

- [1] H. Kimura, Hydrogen sulfide: its production, release and functions, *Amino Acids* 41 (2011) 113–121.
- [2] L. Li, P. Rose, P.K. Moore, Hydrogen sulfide and cell signaling, *Annu. Rev. Pharmacol. Toxicol.* 51 (2011) 169–187.
- [3] R.A. Dombkowski, M.J. Russell, K.R. Olson, Hydrogen sulfide as an endogenous regulator of vascular smooth muscle tone in trout, *Am. J. Physiol. Regul. Integr. Comp. Physiol.* 286 (2004) R678–R685.
- [4] Y. Kaneko, Y. Kimura, H. Kimura, I. Niki, *L*-Cysteine inhibits insulin release from the pancreatic β -cell: possible involvement of metabolic production of hydrogen sulfide, a novel gasotransmitter, *Diabetes* 55 (2006) 1391–1397.
- [5] R.C.O. Zanardo, V. Brancalione, E. Distrutti, et al., Hydrogen sulfide is an endogenous modulator of leukocyte-mediated inflammation, *FASEB J.* 20 (2006) 2118–2120.
- [6] K. Eto, T. Asada, K. Arima, T. Makifuchi, H. Kimura, Brain hydrogen sulfide is severely decreased in Alzheimer's disease, *Biochem. Biophys. Res. Commun.* 293 (2002) 1485–1488.
- [7] P. Kamoun, M.C. Belardinelli, A. Chabli, K. Lallouchi, B. Chadeaux-Vekemans, Endogenous hydrogen sulfide overproduction in Down syndrome, *Am. J. Med. Genet. A* 116A (2003) 310–311.
- [8] W. Yang, G. Yang, X. Jia, L. Wu, R. Wang, Activation of KATP channels by H_2S in rat insulin-secreting cells and the underlying mechanisms, *J. Physiol.* 569 (2005) 519–531.
- [9] S. Fiorucci, E. Antonelli, A. Mencarelli, et al., The third gas: H_2S regulates perfusion pressure in both the isolated and perfused normal rat liver and in cirrhosis, *Hepatology* 42 (2005) 539–548.
- [10] C. Szabo, Hydrogen sulphide and its therapeutic potential, *Nat. Rev. Drug Discov.* 6 (2007) 917–935.
- [11] H. Peng, W. Chen, S. Burroughs, B. Wang, Recent advances in fluorescent probes for the detection of hydrogen sulfide, *Curr. Org. Chem.* 17 (2013) 641–653.
- [12] A.R. Lippert, Designing reaction-based fluorescent probes for selective hydrogen sulfide detection, *J. Inorg. Biochem.* 133 (2014) 136–142.

- [13] V.S. Lin, C.J. Chang, Fluorescent probes for sensing and imaging biological hydrogen sulfide, *Curr. Opin. Chem. Biol.* 16 (2012) 595–601.
- [14] N. Kumar, V. Bhalla, M. Kumar, Recent developments of fluorescent probes for the detection of gasotransmitters (NO, CO and H₂S), *Coord. Chem. Rev.* 257 (2013) 2335–2347.
- [15] T. Chen, Y. Zheng, Z. Xu, et al., A red emission fluorescent probe for hydrogen sulfide and its application in living cells imaging, *Tetrahedron Lett.* 54 (2013) 2980–2982.
- [16] Y. Zheng, M. Zhao, Q. Qiao, et al., A near-infrared fluorescent probe for hydrogen sulfide in living cells, *Dyes Pigments* 98 (2013) 367–371.
- [17] Y.H. Li, J.F. Yang, C.H. Liu, J.S. Li, R.H. Yang, Colorimetric and fluorescent detection of biological thiols in aqueous solution, *Chin. Chem. Lett.* 24 (2013) 96–98.
- [18] Q. Liu, L. Xue, D.J. Zhu, G.P. Li, H. Jiang, Highly selective two-photon fluorescent probe for imaging of nitric oxide in living cells, *Chin. Chem. Lett.* 25 (2014) 19–23.
- [19] S. Wu, Y.J. Wei, Y.B. Wang, et al., Ratiometric and selective two-photon fluorescent probe based on PET-ICT for imaging Zn²⁺ in living cells and tissues, *Chin. Chem. Lett.* 25 (2014) 93–98.
- [20] X.H. Yang, S. Sun, P. Liu, et al., A novel fluorescent detection for PDGF-BB based on dsDNA-templated copper nanoparticles, *Chin. Chem. Lett.* 25 (2014) 9–14.
- [21] H. Zheng, X.Q. Zhan, Q.N. Bian, X.J. Zhang, Advances in modifying fluorescein and rhodamine fluorophores as fluorescent chemosensors, *Chem. Commun.* 49 (2013) 429–447.
- [22] X. Chen, T. Pradhan, F. Wang, J.S. Kim, J. Yoon, Fluorescent chemosensors based on spiroring-opening of xanthenes and related derivatives, *Chem. Rev.* 112 (2011) 1910–1956.
- [23] G.M. van Dam, G. Themelis, L.M.A. Crane, et al., Intraoperative tumor-specific fluorescence imaging in ovarian cancer by folate receptor- α targeting: first in-human results, *Nat. Med.* 17 (2011) 1315–1319.
- [24] V. Dujols, F. Ford, A.W. Czarnik, A long-wavelength fluorescent chemodosimeter selective for Cu(II) ion in water, *J. Am. Chem. Soc.* 119 (1997) 7386–7387.
- [25] Z.X. Han, B.S. Zhu, T.L. Wu, et al., A fluorescent probe for Hg²⁺ sensing in solutions and living cells with a wide working pH range, *Chin. Chem. Lett.* 25 (2014) 73–76.
- [26] C. Liu, J. Pan, S. Li, et al., Capture and visualization of hydrogen sulfide by a fluorescent probe, *Angew. Chem. Int. Ed.* 50 (2011) 10327–10329.
- [27] J. Zhang, Y.Q. Sun, J. Liu, Y. Shi, W. Guo, A fluorescent probe for the biological signaling molecule H₂S based on a specific H₂S trap group, *Chem. Commun.* 49 (2013) 11305–11307.
- [28] C. Wei, Q. Zhu, W. Liu, et al., NBD-based colorimetric and fluorescent turn-on probes for hydrogen sulfide, *Org. Biomol. Chem.* 12 (2014) 479–485.
- [29] C. Liu, B. Peng, S. Li, et al., Reaction based fluorescent probes for hydrogen sulfide, *Org. Lett.* 14 (2012) 2184–2187.
- [30] T. Liu, Z. Xu, D.R. Spring, J. Cui, A lysosome-targetable fluorescent probe for imaging hydrogen sulfide in living cells, *Org. Lett.* 15 (2013) 2310–2313.
- [31] T. Liu, X. Zhang, Q. Qiao, et al., A two-photon fluorescent probe for imaging hydrogen sulfide in living cells, *Dyes Pigments* 99 (2013) 537–542.